Extended Abstracts of the 2018 International Conference on Solid State Devices and Materials, Tokyo, 2018, pp705-706

Multifunctional Black Phosphorus Lateral Heterojunction for Optoelectronics

Lin Wang[1,2], Li Huang[1,2], Wee Chong Tan[1,2], Xuewei Feng[1,2], Li Chen[1,2] and Kah-Wee Ang[1,2,*]

[1] Department of Electrical and Computer Engineering, National University of Singapore, 4 Engineering Drive 3, Singapore 117582
[2] Centre for Advanced 2D Materials, National University of Singapore, 6 Science Drive 2, Singapore 117546
[*] Phone: +65 6516-2575, Fax: +65 6779-1103, Email: eleakw@nus.edu.sg

Abstract

Here, we report an electrically tunable black phosphorus (BP) lateral heterojunction for high-performance optoelectronic application. The device exhibits a significant gate-tunable current-rectifying behavior. It shows great potential for infrared photodetection with 235 A/W photoresponsivity and <10^{-2} pW/Hz$^{1/2}$ shot noise equivalent power demonstrated at 1550 nm, the highest and lowest values reported for BP-based photodetectors at this wavelength. In parallel, it can be used for light energy harvesting in both visible and near-infrared regimes, beyond the bandgap limitation of transition metal dichalcogenides (TMDCs). This work paves the way for the exploitation of BP lateral heterojunction for broadband energy harvesting and photodetection with enhanced performance.

1. Introduction

Recent years have witnessed inspiring research progress in realizing both lateral and vertical p-n junctions using two-dimensional (2D) materials for optoelectronic applications, with significant focus on electrostatically defined van der Waals structures. However, despite the inherent nature of band gap dependence on 2D crystal layer thickness, few works have been done on exploring the potential of naturally-formed lateral heterojunctions. BP exhibits a prominent thickness-dependent bandgap ranging from 2.0 eV for monolayer to 0.3 eV for bulk, which implies the existence of appreciable band discontinuity at the interfaces with BP layer-number differences, offering the opportunity to form heterostructures for optoelectronic applications with superior performance.

2. Device Structure and Fabrication

A schematic of the device is shown in **Fig. 1a**. BP flakes were mechanically exfoliated onto a p^{++}-doped Si substrate covered with 90 nm SiO_2. Optical microscope was used to identify flakes of interest that contain attractive thickness variation. An optical image of the flake for device fabrication is given in the inset of **Fig. 1b** showing apparent color contrast between different flake thicknesses. Then 3 nm/60 nm Ni/Au electrodes were formed using laser lithography and sputtering followed by a standard lift-off process. Finally, 20 nm Al_2O_3 was grown by ALD to serve as passivation layer. The BP thicknesses for three regions are revealed by AFM to be 6.1 nm (region I), 3.3 nm (region II), 5.0 nm (region III), respectively, which are likely to form heterojunctions at their interfaces as a result of their different bandgaps. Here, we report the characterization of the device containing area I and II.

3. Results and Discussion

The device exhibits a typical ambipolar behaviour dominated by hole conduction **(Fig. 2a)** and a current on/off ratio of ~10^6 is obtained, with an ultralow off-state current density of 8 pA/μm (for 0.1 V V_d). The high on/off ratio and small off-current were ascribed to the thinner portion of the channel leading to a larger bandgap and a more efficient gate control. From output characteristics (I_d-V_d) in **Fig. 2b**, significant rectifying behavior is observed for a certain V_g range between 10 V and 40 V, indicating good heterojunction diode formation.

Fig. 3a shows the measured photocurrent (I_{ph}=$I_{d,light}$ - $I_{d,dark}$,) as a function of V_g at a fixed 1 V V_d at various excitation laser power (1550 nm). The corresponding dark current curve is also provided in the lower panel. Evidently, the device exhibits a good gate-tunable photocurrent characteristic with the maximum I_{ph} obtained at the device on-state. To better study the gate-dependent photocurrent generation, we extract its values at three typical V_g (0 V, 20 V, 30 V) and plot it as a function of laser power (**Fig. 3b)**. The photocurrent in the device on-state is almost three orders of magnitude higher than in its off-state, as a result of distinct photocurrent generation mechanism between photogating effect and photoconductive effect.

The responsivity is calculated by using the equation R=I_{ph}/P_{in}, where P_{in} is the incident light power on the device area. Inspiringly, a responsivity as high as 235 A/W is achieved at 1.8 nW incident laser power and 0 V V_g (**Fig. 3c**), which is by far the highest responsivity for all-BP-based photodetectors in the 1-4 μm infrared range, including those with BP-based vertical heterostructures (**Fig. 4a**).

We also calculate the inferred noise equivalent power (NEP=noise/R) and detectivity (D*) of the device. In **Fig. 3b**, the gate-dependent shot-noise-limited NEP of our device (NEP_{shot}) is under 10^{-1} pW/Hz$^{1/2}$ over the full V_g range and reaches as low as 5.5×10^{-3} pW/Hz$^{1/2}$ at 20 V V_g, rendering it the smallest compared with previously reported values for traditional BP phototransistors (**Fig. 3c**), implying great potential for ultralow power detection. Based on the calculated NEP, a detectivity of 5.2×10^{10} Jones is achieved (**Fig 4d**) at room temperature at V_g=20 V and V_d=2 V, which is well comparable to the state-of-the-art PbS infrared photodetectors. Considering the room for further performance improvement by thickness optimization, BP heterojunction transistor is likely to make a competitive candidate for future photodetector application.

In addition to photodetection under external V_d, the heterojunction transistor also enables infrared photodetection at zero V_d, owing to its built-in electrical field, which does not existing in conventional BP transistors. **Fig. 5a** shows gate-tunable photocurrent under varying laser power at 1550 nm. **Fig. 5b** and **5c** display I_{ph} versus P_{in} at 36 V V_g and time-domain response of the device, respectively. The responsivity is calculated to be 4.3 mA/W. Furthermore, by tuning gate bias, the device can readily be used for light energy harvesting both in visible and infrared regimes. In **Fig. 6a**, the I_d-V_d curve passes through the fourth quadrant and shifts downward with increasing light power, implying a photovoltaic process occurring inside a heterojunction. The produced electrical power can be evaluated using the equation P_{el}=-V_d·I_d. In **Fig. 6b**, a maximum P_{el} of 80 pW is obtained at 110 mV V_d for 379 nW P_{in}. By assuming 300 nm active region near the hetero-interface, the power conversion efficiency of 0.25% (η=$P_{el,m}$/P_{in}) can be determined, which is better than the local-gate defined and chemically doped BP p-n junction.

4. Conclusions

We have demonstrated the potential of a gate-tunable BP heterojunction phototransistor for high-performance infrared photodetection. Moreover, the device can operate as a photovoltaic diode, enabling its application for zero-V_d photodetection and light energy harvesting. This work expands the realm of BP and 2D materials for future optoelectronic devices with enhanced performance.

References

[1] N. Youngblood *et al.* Nat. Photonics **9** (2015) 247. [2] Q. Guo *et al.* Nano Lett. **16** (2016) 4648. [3] Huang, L. *et al.* ACS Appl. Mater. Interfaces **9** (2017) 36130. [4] Xu, M. *et al.* Appl. Phys. B. **123** (2017) 130. [5] Engel, M *et al.* Nano Lett. **14** (2014) 6414. [6] C. Chen *et al.* Nano Lett. **17** (2017) 985. [7] H. Yuan *et al.* Nat. Nanotechnol. **10** (2015) 707. [8] X. Yu *et al.* Nano Energy **25** (2016) 34. [9] J. Jia *et al.* Chem. Mater. 29 (2017) 3143. [10] L. Ye *et al.* Nano Energy **37** (2017) 53. [11] L. Wang *et al.* Adv. Electron. Mater. **4** (2018), 1700442. [12] M. Buscema *et al.* Nat. Commun. **5** (2014) 651. [13] Y. Liu *et al.* Adv. Funct. Mater. **27** (2017) 1604638.

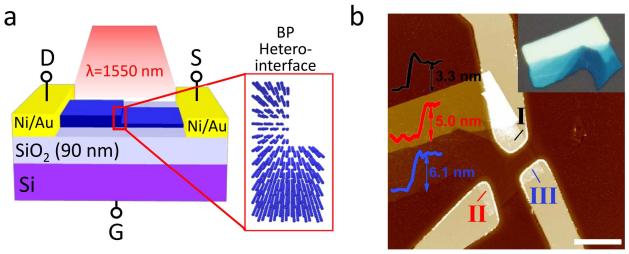

Fig. 1. Structural properties of BP lateral heterojunction device. (a) Schematic of thickness-modulated BP heterojunction transistor. (b) Topography image of the device after fabrication from AFM tapping scan. Scale bar is 5 µm. Inset is an optical micrograph of the BP sheet after exfoliation, showing clear contrast between regions of different BP thickness.

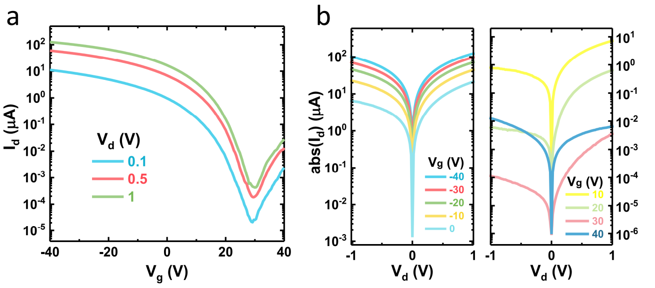

Fig. 2. (a) Transfer characteristics of device at different V_d biases, showing hole-dominant conduction behaviour. It displays a gate-modulating on/off ratio of ~10^6 and the off-state current density reaches as small as 61 pA/ µm. (b) I_d-V_d characteristics of device at various V_g values, showing evident current rectification in the 10 to 40 V range, indicating the existence of rectifying junction.

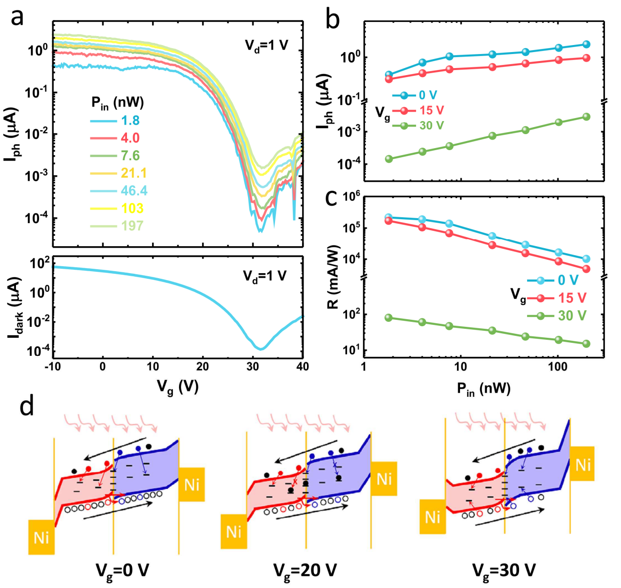

Fig. 3. Tunable photoresponse of BP heterojunction phototransistor at 1550 nm and 1 V V_d. (a) Bottom: I_d as a function of V_g in the dark condition. Top: Gate-dependent photocurrent (I_{ph}) under varying light power. (b) Extracted I_{ph} at typical V_g values as a function of excitation power. (c) Calculated photoresponsivity (R) at typical V_g values and its dependence on light power. (d) Energy band diagram of BP heterojunction to illustrate photocurrent generation mechanism of the device at different operating conditions.

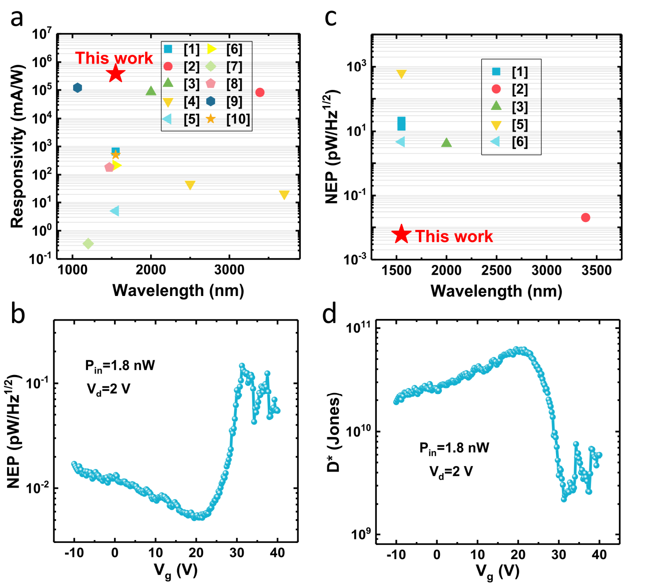

Fig. 4. (a) Responsivity of BP heterojunction phototransistor at 1550 nm compared with reported values of all-BP-based infrared (1-4 µm) photodetectors. (b) Calculated NEP_{shot} as a function of V_g under 1.8 nW P_{in} at V_d=2 V. The smallest NEP_{shot} reaches 5.5×10^{-3} pW/Hz$^{1/2}$ near 20 V V_g. (c) Comparison of NEP_{shot} between the BP-heterojunction device in this work with reported BP-based photodetectors. (d) Calculated detectivity of BP heterojunction phototransistor in dependence of V_g for V_d=2 V. A highest value of 6.2×10^{10} Jones is obtained near 20 V V_g.

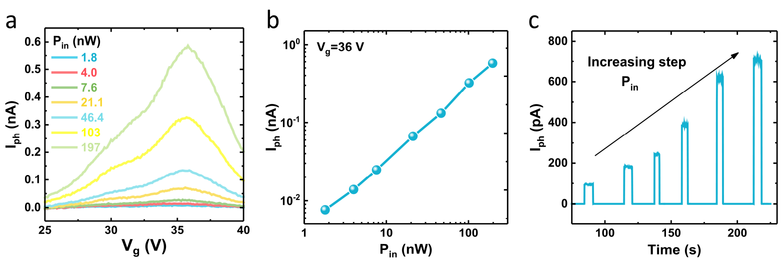

Fig. 5. BP heterojunction transistor for infrared photodetection at zero V_d. (a) Gate-dependent photocurrent arising from BP heterojunction transistor under varying laser powers with zero external V_d applied. (b) Extracted photocurrent and photoresponsivity in dependence of P_{in}. Inset shows the photocurrent generation process owing to the built-in electrical field within the heterojunction. (c) Time domain photoresponse of the device under increasing laser power steps.

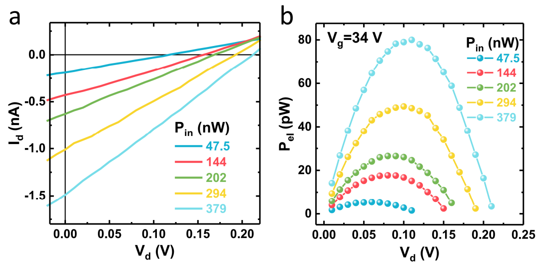

Fig. 6. Gate-tunable photovoltaic effect in BP-based heterojunction at 660 nm. (a) I_d-V_d characteristics of the device under various illumination situations at V_g=34 V, showing evident photovoltaic behavior. (b) Generated electrical power of BP heterojunction device as a function of V_d under different incident light power P_{in}.

Acknowledgement: This research was supported by A*STAR Science and Engineering Research Council Grant (No. 152-70-00013), National Research Foundation Competitive Research Program (NRF-CRP15-2015-02), and by the National Research Foundation, Prime Minister's Office, Singapore under its medium sized center program.